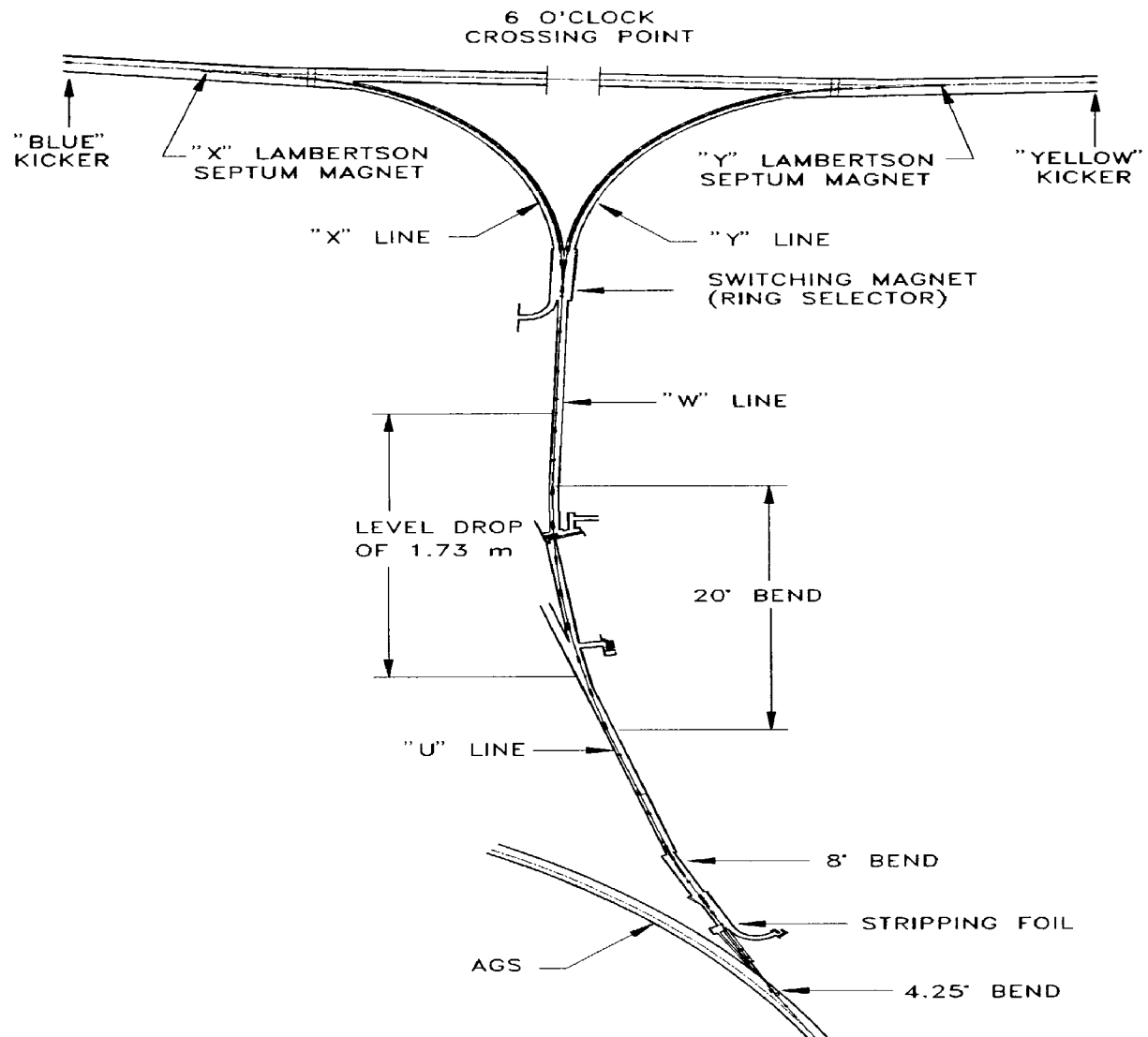


## ii. Equipment

AGS extracted beam bunches pass through a transfer line in moving from AGS to RHIC, a layout of which appears as Fig. 5-1. The transfer line is called the ATR (AGS To RHIC) line, and begins downstream of AGS extraction which comprises a new G10 Extraction Kicker and new H10 Extraction Septum. Before exiting the AGS vault, the beam undergoes a  $4.25^\circ$  bend through two dipole magnets accompanied by three quadrupoles. The bunches then traverse a spur called the "U" line, which had been in operation for many years for the AGS neutrino program. The old "U" line has been dismantled, and all components have been either re-furbished or replaced for ATR operation.

An  $8^\circ$  dispersion free bend comprised of four gradient dipoles connected in a modified triplet (FDDF) configuration is found in the "U" line. Prior to the  $8^\circ$  bend, a stripping station is located where the last two electrons are removed from the as yet not fully stripped heaviest species. The stripper can be retracted when it is not needed. Transport optics are designed to form a double waist at the foil to minimize the dilution in phase space of the beam caused by scattering in the foil and to compensate for the associated changes in emittance shape. This first section of the ATR will be shared, at least for the next few years of operation, with the g-2 AGS experiment, and optic components were chosen to accommodate the differing transport requirements. A pair of g-2 deflection magnets (VD3 and VD4) are located just upstream of the  $8^\circ$  bend. Activation of the deflection magnet pair will direct beams to the g-2 target for the AGS experimental program; deactivation allows RHIC injection. Changeover from high intensity protons for g-2 to RHIC beams should be on the order of 1/2 hour for the beamline retuning. Six quadrupoles preceding and four following the  $8^\circ$  bend allow tuning capability to prepare the bunches for acceptance into the subsequent "W" line spur.

This next section of the beam transfer line, the "W" line, deflects the beam both horizontally and vertically, such that its axis at the entrance to the ring selector runs along the intersection of a horizontal plane, approximately 48 mm above RHIC's median plane, and the vertical plane through the machine center and the crossing point at 6 o'clock. This vertical plane is a plane of reflection symmetry: reflecting one ring and its beam transfer branch in it yields the other.



**Fig. 5-1.** Schematic layout of the AGS to RHIC (ATR) transfer line.

The horizontal deflection in this section is  $20^\circ$  in an arc with an average radius of 405.82 m, the change in vertical level is approximately 1.73 m. The horizontal deflection and the change in level are entwined: the former is performed by a string of 8 gradient magnets in an AG focusing arrangement, the latter by a pair of vertical pitching dipoles, the first one of which is located between the second and third horizontal deflectors. The gradient magnets are each about 3.66 m long with a field strength of about 1.19 T. They are separated from each other by drift spaces of 14.05 m. The second pitching dipole is placed between the second and third quadrupole of a string of six between the last horizontal deflector and the switching magnet (ring selector). These, together with the upstream quadrupoles in the "U" line, provide for flexibility in the choice of focusing parameters at the entrance of the ring selector. Between the second pitching magnet and the switching magnet, the beam line can be nominally free of horizontal and vertical dispersion ( $X_p = X'_p = 0$  and  $Y_p = Y'_p = 0$ ), thus ensuring reflection-symmetric behavior of the beam in the subsequent beam transfer branches into the two rings. The final drop in beam level over about 48 mm in the injection region leaves a small residual vertical dispersion in the circulating beam, thus increasing the vertical emittance by a small amount. This increase can be avoided altogether by resetting the system to compensate for that dispersion.

The next sections consist of the two reflection-symmetric branches which begin at the entrance to the switching magnet and end in the injection halls. The switching magnet guides the beam via a dispersion match into one of these two "big bend" strings of 25 long plus 1 short gradient magnets, which carry the beam along arcs with average radii of 96.333 m and deflection angles of 48.15 mrad in each long gradient magnet. The gradient magnets in each big bend are arranged in a OFoFOODO pattern with horizontal and vertical betatron phase advances of about  $\pi/2$  rad per cell.

Each big bend ends in its associated injection hall in the 6 o'clock insertion as shown in Fig. 5-2. There it is followed by a matching section, a string of four horizontally deflecting gradient magnets, one horizontally deflecting dipole, and six quadrupoles which are located and excited to match the betatron functions and the dispersion functions of the transfer line to those of the RHIC lattice upstream of the RHIC quadrupole Q8O. The five bending magnets will each be about 2.95 m long, and together will deflect the beam through about

**Table 5-1.** Injection Magnet Parameters

	Kicker	Septum
Deflection (mrad)	1.86	38
Strength (T·m) @ $B\rho = 100$ T·m	0.186	3.8
Field (T)	0.044	0.95
Length (m)	4×1.12	4.0
Beam tube aperture, i.d. (mm), circulating beam H×V (mm), incoming beam	41.2	67.4 63.5×26.1
Risetime (1 - 99%) (nsec)	95	
Flat top (nsec)	20	
Flat top tolerance	±1%	
Fall time (nsec)	800	

198 mrad. Three of the six quadrupoles for adjustment of the match between big bend and RHIC are imbedded into this string, the other three form a triplet at the end of the string. Injection occurs downstream of the last transfer line triplet, YQ4, YQ5 and YQ6 in Fig. 5-2. The injected beam lies in a plane vertically about 48 mm above the collider ring midplane. A vertical deflection ( $\sim 3$  mrad) is provided by the pitching dipole magnet (YP1), upstream of the septum, to direct the incident beam downward through the RHIC quadrupoles Q8O and Q9O, so that it will cross the RHIC reference orbit in the center of the injection kicker magnet located downstream of Q9O. The arrangement of the injection magnets is shown in Fig. 5-3 and their principal parameters are listed in Table 5-1.

An iron septum (Lambertson) magnet, bending 38 mrad horizontally, brings the incident beam axis into coincidence, horizontally, with the reference orbit in the outer arc. The iron septum of the Lambertson magnet separates the incident beam from the circulating one. In the region of the circulating beam, the stray field from the septum is held to less than 0.2 G by means of a soft-iron beam pipe, acting as a magnetic shield. The insertion CQS assemblies Q8O and Q7O will be shortened in this region by omitting the blank sextupole correctors, in order to allow sufficient space for the incoming beam to clear the ring components.

Leaving the septum the beam passes off-axis through the aperture of the vertically defocusing ring quadrupole Q8O, and the vertically focusing Q9O, and is finally bent into the median plane by injection kickers KI1 - KI4. The four injection kicker modules provide a vertical deflection of 1.86 mrad, depositing the beam onto the RHIC orbit.

### The Septum Magnet

The Iron Septum (Lambertson) Magnets are designed to horizontally deflect the injected beam onto a path parallel to the circulating beam. Two such magnets are used, each one injecting into one of the counter-circulating beams of the RHIC machine. The two magnets are identical magnetically, but are physically mirror images of each other. The Septum Magnet is the last element in the ATR beam transfer line and is electrically in series with the transfer line dipoles, thus saving the cost of a separate large power supply; a separate trim power supply is connected in parallel across the septum magnet to allow fine adjustment of the injection angle.

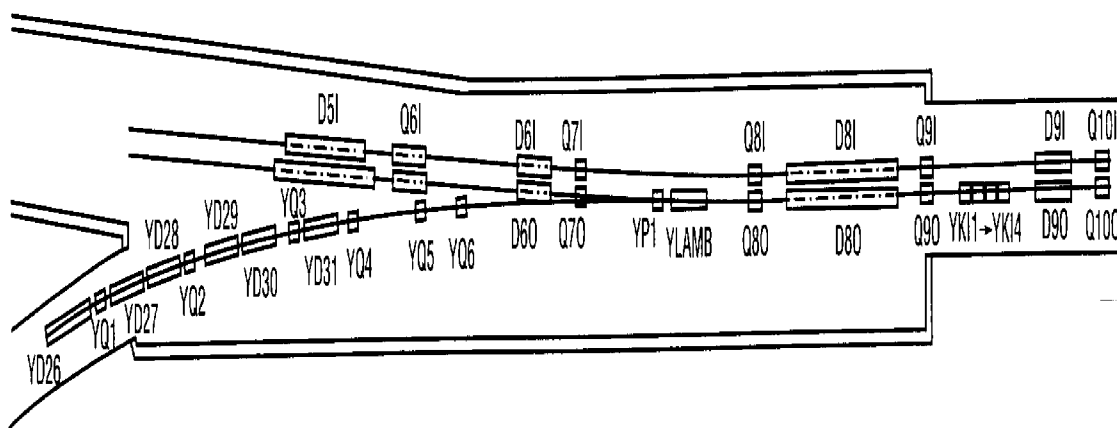


**Fig. 5-2.** Six o'clock insertion with location of yellow ring injection equipment.

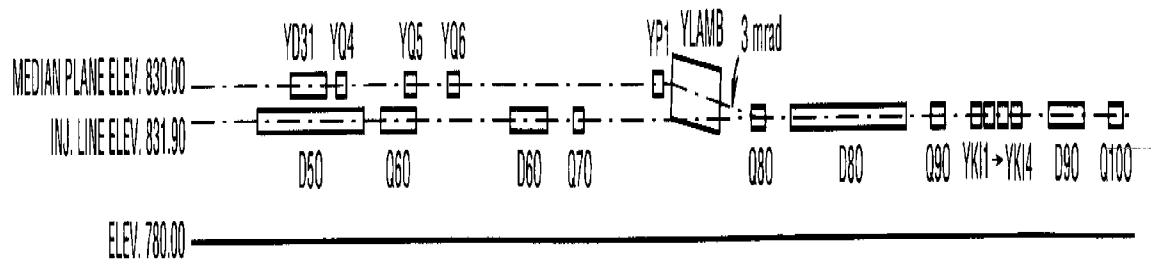


**Fig. 5-3.** Injection component layout/(elevation).

**Table 5-2.** Septum Magnet Parameters

Bend angle @ $B\rho = 100 \text{ T}\cdot\text{m}$	38	mrاد
Length		4 m
Magnetic field @ injected beam		9.5 kG
Field uniformity @ injected beam		$< 6\times 10^{-4}$
Stray fields @ circulating beam		$< 0.2 \text{ G}$
H/V aperture @ injected beam		$63.5\times 26.1 \text{ mm}^2$
Wall thickness @ injected beam tube		0.8 mm
Beam tube i.d. @ circulating beam		67.4 mm
Wall thickness @ circulating beam tube		1.3 mm
Septum thickness		10.8 mm
Vacuum requirement	$< 1\times 10^{-10}$	mbar

The magnets are designed to achieve field uniformity of  $\Delta B/B < 6\times 10^{-4}$  over the width of the incident beam path and stray fields in RHIC's circulating beam pipe of less than 0.2 G at  $B_0 = 9.5 \text{ kG}$  transverse to the beam direction. In addition, the magnet is ultra-high vacuum compatible in that only the insides of the beam tubes are exposed to the vacuum and the entire assembly is bakeable in situ to 300 °C. The principal design parameters are listed in Table 5-2.

The relative location of the magnet with respect to the straight section Q7O - Q8O of the RHIC ring is shown in Fig. 5-4a (top view), 5-4b (side view), and 5-4c (view looking upstream). Figure 5-4a shows the injected beam at the entrance of the magnet which will bend by  $\sim 38 \text{ mrad}$  and will then continue at the exit of the magnet on the same vertical plane as the RHIC circulating beam.

The geometry of the magnet changes along the beam axis; one of the cross sections of the magnet is shown in Fig. 5-5 and corresponds to the middle of the magnet. A dimensioned view of the "Y" line injection area, indicating the Lambertson and ancillary devices, is presented in Fig. 5-6.

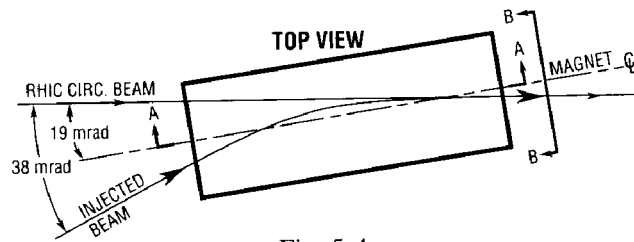


Fig. 5-4a.

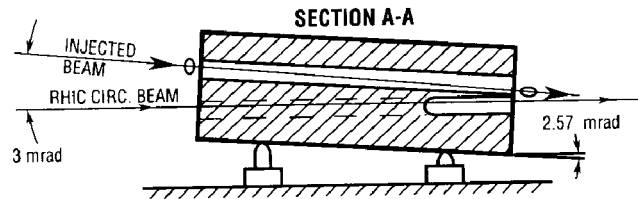


Fig. 5-4b.

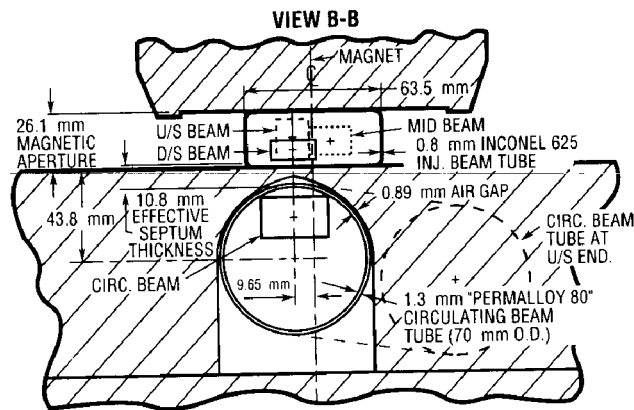


Fig. 5-4c.

Fig. 5-4. Septum Magnet.

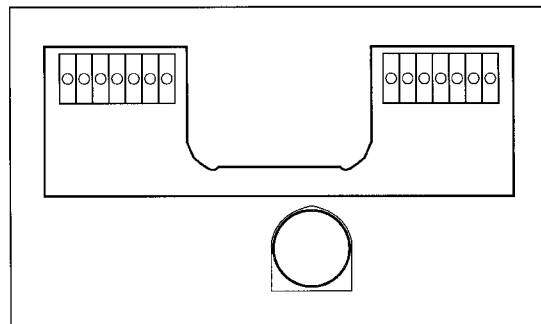


Fig. 5-5. Septum Magnet Cross Section.



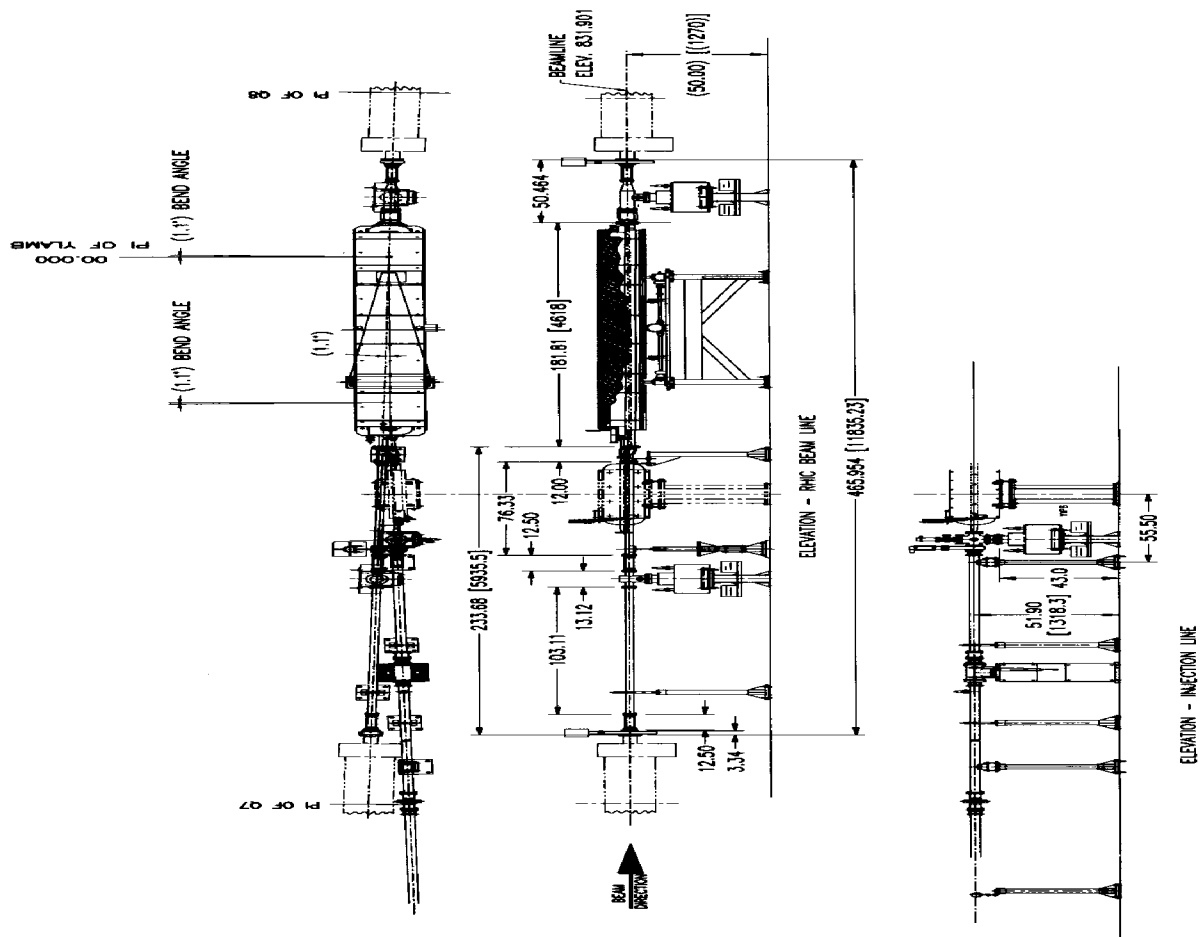
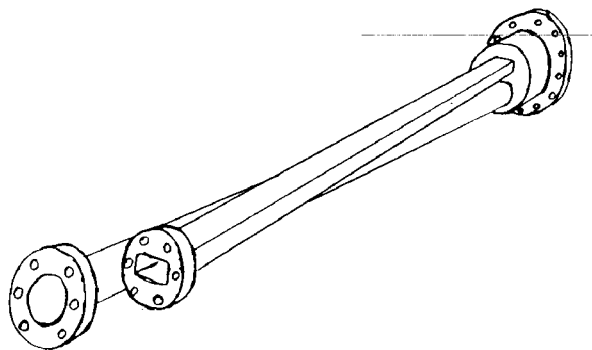


Fig. 5-6. "Y" line Lambertson injection area. (Brackets show dimensions in mm)

*Steel Characteristics.* Two and three-dimensional computer modeling showed that the design parameters could be met and exceeded by fabricating the magnet body out of an ultra-low carbon ( $< 0.005\%$ ) steel in the unannealed condition. The material (called "INTRAK") is available in large slabs and can be machined without significantly altering the magnetic properties.

*Beam tube Materials.* The material for the circulating beam tube is critical as it serves a number of functions. First, it must be ultra-high vacuum compatible, which means prefiring at a temperature of at least  $950\text{ }^{\circ}\text{C}$  in a vacuum of at least  $1 \times 10^{-5}$  mbar and should be corrosion-free like stainless steel. In addition, it serves a vital magnetic shielding function. The tube is spaced from the surrounding ultra-low carbon steel by a 1 mm air gap and intercepts leakage fields. For this function, it must have high permeability at low field levels. It must also have sufficient physical strength to resist the vacuum loads with a relatively thin wall. Finally, it helps if the thermal coefficient of expansion is close to that of the magnet body. These conditions are all met by a material called "Permalloy 80." To reach the required annealed condition, it must be heated to  $1150\text{ }^{\circ}\text{C}$  after fabrication. This also serves as the vacuum firing.

The injection tube material selected is Inconel 625. It is completely non-magnetic, has good vacuum and thermal expansion properties, and has high stiffness and yield strength to resist vacuum loading. Both the beam tubes are welded into the common stainless steel downstream chamber (see Fig. 5-7).



**Fig. 5-7.** Septum Magnet Vacuum Chamber.

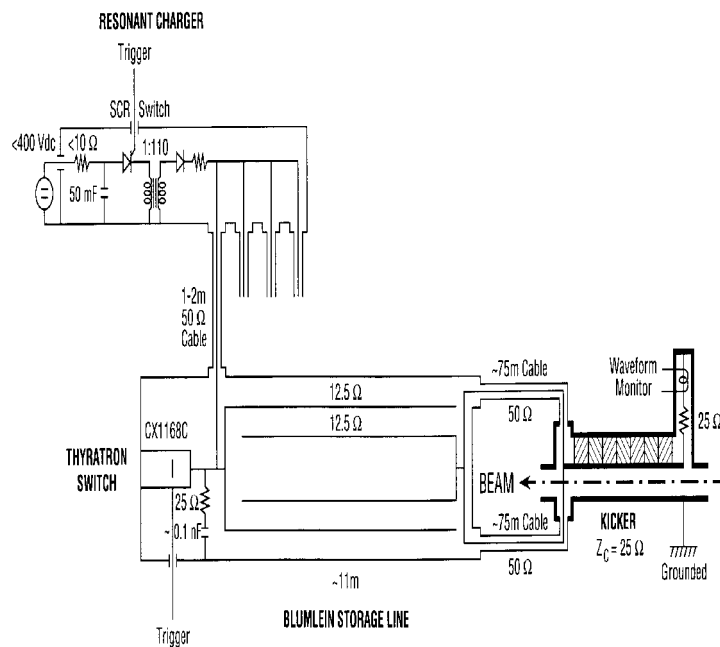
*Bakeout.* Because of the difficulty of trying to heat the injection tube (which is in intimate contact with the poles) independently of the magnet, it was decided to heat the entire magnet. The coil is thermally insulated from the core and is water cooled during bakeout. A covering heater blanket of 20 kW heats the assembly to 250 °C in 12 hours.

*Vertical Motion.* During injection, the magnet must be positioned so that the circulating beam almost touches the upper inside surface of the circulating beam tube. This condition represents an aperture restriction for the RHIC machine during the subsequent operating cycle. To solve this problem, provision has been made to raise the entire magnet, after injection, so that the center lines of the circulating beam tube and the circulating beam coincide. This is accomplished to an accuracy of  $\pm 0.1$  mm by coupling the three support jacks to a common motor with suitable position feedback and limit switches.

## Injection Kicker System

The purpose of the injection kicker is to provide the ultimate deflection to the incoming beam from the AGS into RHIC. The beam is kicked in the vertical direction to place it on the equilibrium orbit of RHIC. Each bunch in the AGS is transferred separately and stacked box-car fashion in the appropriate RHIC rf bucket. In order to achieve the required deflection angle, four magnets powered by four pulzers will be used for each ring of RHIC. When the bunches are stacked in RHIC, the last few rf buckets are left unfilled in order to provide a gap in the beam to facilitate the ejection or beam abort process. This also means there is not a severe constraint on the fall-time of the injection kicker. The performance specifications for the kicker are given in Table 5-1. The performance is achieved using four Blumlein pulzers each connected to a magnet forming a matched transmission system. The pulzers will be located outside the RHIC tunnel and will be connected to the magnets by about 75 m of high voltage cable. An overview of the injection kicker system is shown in Fig. 5-8.

**Fig. 5-8.**  
Overview of the  
injection kicker  
system.



*The Kicker Magnet.* The magnet consists of a "C" cross section formed of interspersed ferrite and high dielectric constant bricks to approximate a transmission line as shown in Fig. 5-9. If properly oriented with respect to the beam, both the electric and magnetic fields can contribute additively to the deflecting force, although by far the largest contribution is made by the magnetic field. The characteristics are given in Table 5-3. The dielectric selected has a relative dielectric constant of  $\sim 100$ . This approach greatly reduces the cost usually associated with the machining of capacitance elements required for a transmission line magnet. The use of rectangular bricks of similar dimension, apart from the longitudinal direction, assures easy assembly for potting in epoxy. The drawback to this design approach is the poor high voltage performance. The cross-section shown in Fig. 5-9 illustrates the problem: the high voltage conductor fits into the rectangular corners of ferrite/dielectric "C" magnet but, despite shaping the conductor, the local electric stress in the corners is very high, particularly in the longitudinal direction in the vicinity of the dielectric sections. The stress is further enhanced in the gap adjacent to the conductor by the difference in dielectric constant between the ceramic brick and the epoxy potting compound.

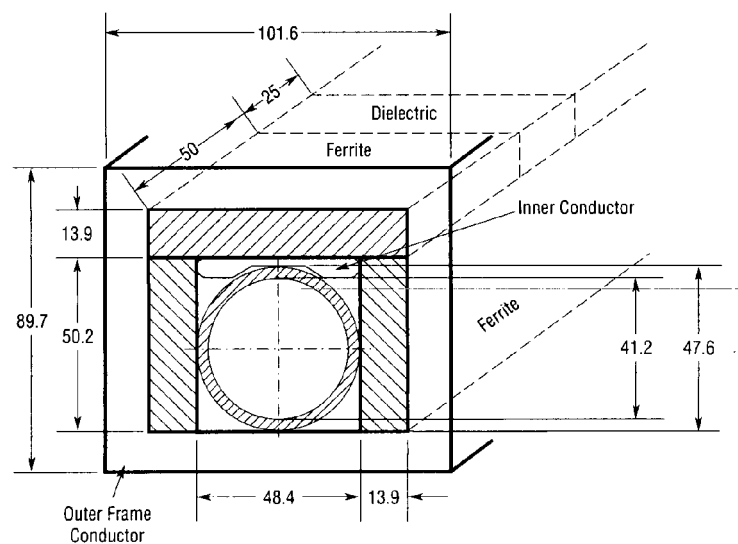


**Fig. 5-9.** RHIC Injection Kicker Geometry (mm)

**Table 5-3. Injection Kicker Magnet Characteristics (each)**

Strength at 2000 A		0.0465 Tm
Number per ring		4
Propagation time		45 ns
Impedance		25 Ω
High frequency cut off		~ 25 MHz
Magnet aperture, width × height		48.4 mm × 51.2 mm
Magnet length	1.12	m
H field deflection		~94%
E field deflection		~ 6%
Ceramic beam tube, circular aperture		41.3 mm
wall thickness		3.2 mm
Min repetition period	33	ms
Life time		10 <sup>6</sup> shots
Core material-ferrite, 15 sections		Ceramic magnetic CMD 5005 50 mm long × 13.9 mm thick
Core material-dielectric, 14 sections		Trans-Tech MCT-100 25 mm long × 13.9 mm thick
Bus bar/return frame	Aluminum 6061-T6	
Epoxy potting material		Conap Inc RN1000

A clear epoxy (RN1000 from Conap) gives the best results. A gap of 0.7 mm between the bricks can be inspected during and after the pour to ensure no voids exist. RN1000 has low viscosity, a long pot life below 22 °C and only 0.8% shrinkage during cure. The magnet is designed to permit high temperature bakeout of the ceramic beam tube. For this procedure, the bottom plate shown in Fig. 5-10 is removed and the magnet elevated above the beam tube. The finite elements comprising the magnet result in a frequency cut off in the 25 MHz range: This increases the effective current risetime to about 40 ns. The combination of risetime and propagation time results in an integrated field risetime of about 85 ns.

*The pulser.* The Blumlein pulser consists of rigid, oil filled transmission lines in a folded, triaxial configuration of the type developed at SLAC. The major dimensions of the storage lines are given in Table 5-4. The triaxial delay line pipes are insulated with Teflon spacers and filled with Calumet Caltran 60-15 oil under slight positive pressure. The dielectric constant is 2.35. The delay lines are assembled from sections each about 2.4 m in length. The combination provides two delay lines of  $12.5\ \Omega$  impedance which feed a  $25\ \Omega$  load formed by the connecting cables ( $2 \times 50\ \Omega$  in parallel), the magnet and a  $25\ \Omega$  oil-filled hockey puck resistor assembly. The electrical properties of the Blumlein are shown in Table 5-4. The pulser is switched by a two-gap deuterium thyatron designed for high  $di/dt$  applications (EEV type CX 1168C). An R-C network in parallel with the switch tube provides a small amount of overshoot in the current waveform, this improves the field risetime by a few nanoseconds.

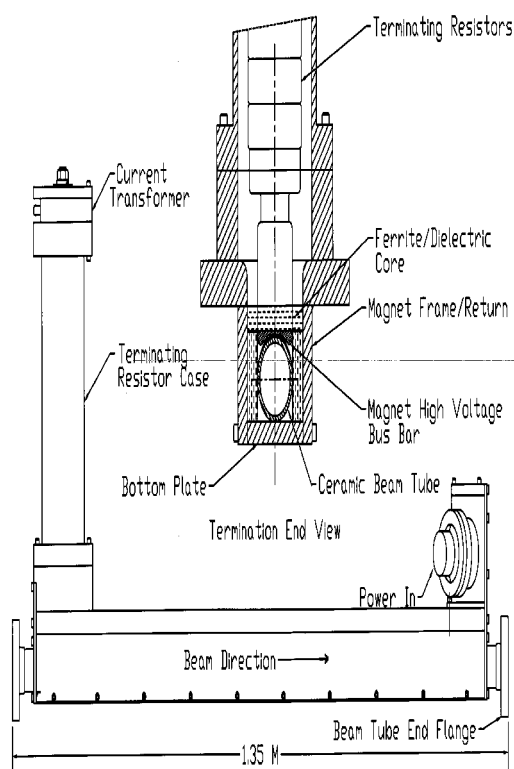


**Fig. 5-10.** General assembly of transmission line magnet.

**Table 5-4.** Blumlein Pulser Parameters

<u>Blumlein Dimensions</u>		
Outer coaxial line	134.5 mm o.d.×98.0 mm i.d. ±0.1	mm
Inner coaxial line	76.2 o.d.×55.5 mm i.d. ± 0.1	mm
Length	10.95	m
Material	Aluminum 6061 - T6	
Insulating oil	Caltran 60-15	
Insulating Standoffs	PTFE Teflon	
<u>Blumlein Pulser Characteristics</u>		
Load impedance	25	Ω
Two-way propagation time	110	ns
Operating voltage	50	kV
Operating load current	2000	A
Max voltage	60	kV
Current risetime	30	ns
Storage line capacitance	10	nF